Advances in ultrasonic testing of austenitic stainless steel welds. Towards a 3D description of the material including attenuation and optimisation by inversion

J. Moysan , C. Gueudré , M.-A. Ploix , G. Corneloup , Ph. Guy , R. El Guerjouma , B. Chassignole

Abstract In the case of multi-pass welds, the material is very difficult to describe due to its anisotropic and heterogeneous properties. Anisotropy results from the metal solidification and is correlated with the grain orientation. A precise description of the material is one of the key points to obtain reliable results with wave propagation codes. A first advance is the model MINA which predicts the grain orientations in multi-pass 316-L steel welds. For flat position welding, good predictions of the grains orientations were obtained using 2D modelling. In case of welding in position the resulting grain structure may be 3D oriented. We indicate how the MINA model can be improved for 3D description. A second advance is a good quantification of the attenuation. Precise measurements are obtained using plane waves angular spectrum method together with the computation of the transmission coefficients for triclinic material. With these two first advances, the third one is now possible: developing an inverse method to obtain the material description through ultrasonic measurements at different positions.

J. Moysan, C. Gueudré, M.-A. Ploix, G. Corneloup

LCND, Université de la Méditerranée, Av. G. Berger, 13625 Aix en Provence, France, joseph.moysan@univmed.fr

Ph. Guy

MATEIS, INSA Lyon, 7 Avenue Jean Capelle, 69621 Villeurbanne, France, philippe.guy@insa-lyon.fr

R. El-Guerjouma

LAUM, Avenue Olivier Messiaen, 72085 Le Mans Cedex 9, France, rachid.elguerjouma@univ-lemans.fr

B. Chassignole

Département MMC, EDF R&D, Site des Renardières, 77818 Moret-sur-Loing, France, bertrand.chassignole@edf.fr

1 Introduction

Austenitic steel multi-pass welds exhibit a heterogeneous and anisotropic structure that causes difficulties in the ultrasonic testing (UT) understanding. Increasing the material knowledge has been an international large and long term research field. Some years ago works aiming at giving a precise description of the material provided significant progresses [1].This paper acquaints firstly with a synthesis of several research works aiming at modelling UT inspection in multipass welds. In all these previous works the UT modelling is considered as 2D case. In a second part the question of a 3D representation of the material resulting from the welding in position arises. New modelling ideas are presented to improve 2D MINA model towards a 3D material description. Modelling is done with the final goal to use inverse methodology in UT testing. The paper syntheses other milestones obtained along this way: attenuation measurements and results with inverse methodology.

2 The context: UT modelling for welds inspection

The main specificity of the weld material is its oriented grain structure which has to be described as an anisotropic and heterogeneous material. The description of the grain structure regularly progresses from simplified and symmetrical structures to more realistic descriptions. Ogilvy [2] proposes to calculate the central ray in a grain structure described by mathematical functions. Schmitz et al [3] use the ray tracing code 3D-Ray-SAFT with an empirical grain structure described by orientation vectors with three coordinates. The EFIT (Element Finite Integration Technique) code is used by Halkjaer et al [4] with Ogilvy's grain structure. Langerberg et al [5] also simulate a simplified symmetrical structure. Spies [6] uses a Gaussian beam approach to calculate the transducer field and to ensure faster modelling. The author simulates the heterogeneity by splitting up the weld into several layers of transverse isotropic material [7]. X. Zhao et al [8] also use a ray tracing approach to determine optimal configuration for flaw detection. Corresponding material descriptions do not always reach the complexity of the heterogeneous structure resulting from manual arc welding. The structure of the real material is non symmetrical and UT modelling may exhibit strong differences [9]. Our modelling approach couples MINA model and ATHENA code [10].
Heterogeneous and anisotropic structure is defined by introducing a mesh containing the grain orientations calculated by MINA model (cf. § 3). This permits to define the appropriate coordinate systems of the elasticity constants at any point of the weld. A result of the coupling between ATHENA and MINA is presented on figure 1. The UT testing is modelled using a 60° longitudinal wave at 2.25 MHz. The corresponding echodynamic curves are calculated using ATHENA results in transmission at the bottom of the weld. In the right part of this figure the result of the coupling MINA-ATHENA is compared with an ATHENA modelling

using the “real” grain structure. This real grain structure is obtained by image analysis of the macrographs [11].

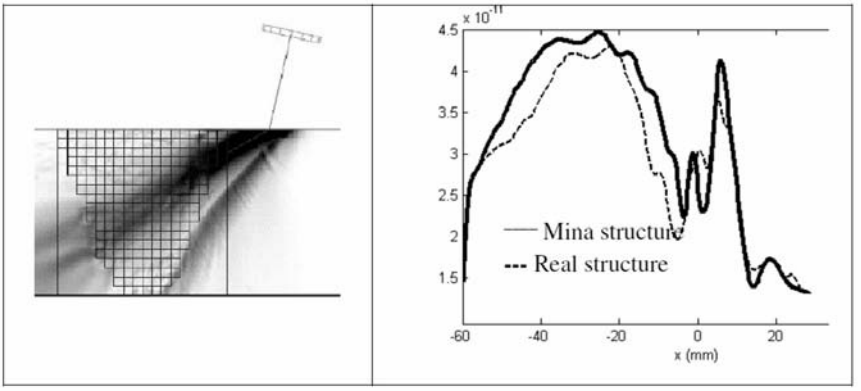

Fig. 1 Example of results from coupling ATHENA and MINA codes.

3 MINA model parameters for flat welding

The MINA model (Modelling anIsotropy from Notebook of Arc welding) was planned to describe the material resulting from flat position arc welding with shielded electrode at a functional scale for UT modeling. It predicts the result of the grain growth [12]. Three physical phenomena are involved: the epitaxial growth, the influence of temperature gradient, and the competition between the grains (selective growth). Epitaxial growth implies that the melt metal takes in each point the crystallographic orientations of the underlying pass. The grain may turn during the growth but the crystallographic orientation is kept. When the temperature gradient changes of direction, grains have a propensity to align themselves with the gradient direction. In the case of multi-pass welding, temperature gradient direction changes within the welding pass and also from one pass to the other. A competition between grains exists as they preferentially grow if their longitudinal axis is close to the direction of the temperature gradient.

The challenge of creating a model reproducing the result of these phenomena has been successfully won with MINA model. The difficulty was to use only knowledge reported in the welding notebook and, in order to complete this knowledge, to find representative parameters of the variation in the deposit of passes. Macrographs analysis was widely used to build the model. The model is dedicated to predict material resulting from flat welding. In that case the grain structure is reputed to be 2D. A complete description of the model can be found in [12]. Main MINA model parameters are recalled here in order to introduce how MINA model may be improved for welding in position. A pass is represented by a parabolic shape. Pass heights are calculated proportionally to the diameters of the

electrodes. A partial remelting is created when a new pass is laid. The two most important parameters are the lateral and the vertical remelting rates, respectively noted R_L and R_V. Two angles are used to imitate the operator's tilt of the electrode. In fact the operator has to modify the way he deposes a pass along the welded joint. This causes an incline of the welding pool. In Figure 2a, weld pool shape and incline of the pass are sketched on a macrograh. Two cases are considered. When a pass leans on the chamfer the angle of rotation θ_B reproduces the influence of the weld geometric chamfer. This angle is considered to be the same for the two sides of the weld due to its symmetry. When a pass leans on a previous pass, the temperature gradient is rotated by an angle noted θ_C. For example in the case where a pass leans to its left and its right on other passes, the angle θ_C equals to zero. All angles are automatically calculated in relation to the location of each pass written in the welding notebook.
With these four parameters (R_L, R_V, θ_B, θ_C) the grain orientation in a mesh is calculated using an algorithm which reproduces the three physical phenomena previously mentioned. The temperature gradient direction is deduced from the parabolic weld pool description [12]. MINA model output is a matrix whose elements represent the local orientation of the grains resulting from the complete solidification process due to the remelting of passes (see figure 2). The matrix elements are calculated pass after pass in the order written down in the book.

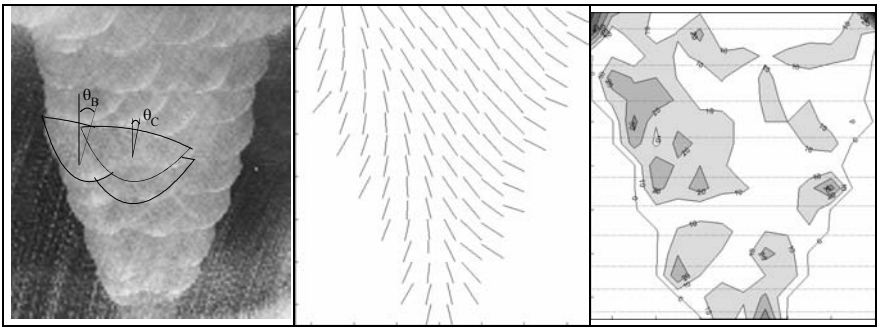

Figure 2. (left to right) Macrographs, resulting grain structure, differences map in the case of an horizontal-vertical weld

4 Improving MINA for welding in position

Welding in position corresponds to several standardized positions: the overhead position, the vertical position (vertical up or vertical down), or the horizontal-vertical position. For this study specific welds have been made with the same base material and the same electrodes. Macrographs were achieved in two perpendicular planes in order to study 3D effects on grain solidification. The conclusions give us clear indications to improve MINA model towards a more

general model: new parameters are then proposed to be able to reproduce grain structure for welds in position. The figure 2 represents one of the new macrographs used for this study. Figure 2b presents resulting grain structure with a mesh-size of 2x2 mm². It could be compared with the corresponding macrograph in Figure 3b. Figure 2c shows the map of orientation differences. Differences are presented with level lines where grain orientations are gathered by about ten degrees. The real grain orientations are measured by an image analysis system. In comparison with previous studies for flat welding position, the resulting of grain structure for horizontal-vertical welding is truly very different. A strong non-symmetrical grain structure can be observed. In figure 2 the differences are localized on the left side of the weld. This demonstrates that the MINA model parameter θ_B which aims at representing the incline of the weld pass on the chamfer could no more be used in the same way as for flat welding (symmetrical behavior). We propose to introduce another parameter called θ_D to take into account this significant difference.

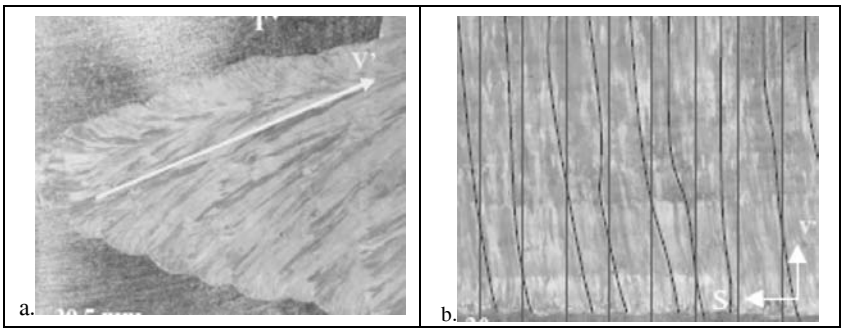

Figure 3. Macrographs of grain structure for horizontal-vertical weld (TV and SV' cuts)

New knowledge is also obtained by considering macrographs in the SV or SV' plane (cf. figure 3b). SV' plane corresponds to a cut along the main grain orientation. These macrographs were done to study disorientations in the welding direction. For flat welding position, no disorientation is observed. A slight disorientation, about 5°, could be observed for welding in overhead position and in horizontal-vertical position. A major one is observed in the case of vertical position welding, it is about 20° to 25°. In figure 3b the grains disorientations were underlined by additional lines following biggest grains. For further studies we propose to introduce a new parameter called Φ corresponding to these disorientations. This parameter should be used to improve the MINA model, but it supposes at first that a fully 3D material is also needed in propagation code.

Another parametric study was done in this work to analyse modelling behaviour when welding in position is considered. The shape of a pass is a very important aspect in the MINA approach as it determines the temperature gradient. The ratio of the width (w) and the height (h) of passes could be an interesting descriptive

parameter to compare passes shape. This ratio w/h is measured on macrographs and could be automatically calculated by MINA. The MINA model gives very satisfactory w/h ratios, with a average difference of 10% with measured ratios on macrographs. The exception is the vertical welding position for which modelled and measured ratios are more different, about 20%. This difference may result from a higher difficulty to estimate with accuracy the remelting parameters on macrographs. If remelting parameters are correct, a modification of the weld pool could be suggested. A large previous experience with macrographs for flat position welding allows assessing that grain structure behaviour is similar if welding conditions keep the same. It enables to conclude that the MINA model could be used with few adaptations for most of the welding positions. In the case of vertical welding, more important differences are observed between the real grain structure and the modelled one. The shape of the weld pool should be modified. For this welding position it would be useful to verify the conclusions on another weld. The most important conclusion for this welding position is the 3D aspect of the grain structure. If this property is not taken into account in modelling, misunderstanding of the UT testing can rapidly occurs. In case of finite element modelling, only 3D codes would correctly predict beam deviation.

5 Attenuation measurements

The second advance which is required for wave propagation codes is a good quantification of the attenuation. The coupling of the MINA-ATHENA codes demonstrated good results when comparing measured and predicted amplitudes at the bottom of the weld (UT in transmission) [10]. Differences are observed when considering the amplitudes. The origin of these differences is the real attenuation, not reproduced with the finite element modelling. The attenuation can reach 0,3 dB/mm for such grain structures [13]. The origin of the attenuation in welded materials is for the most part caused by scattering effect on the columnar grains. The value of this attenuation depends on the size, shape and orientation of the grains. An experimental set up is designed in order to study the ultrasonic attenuation as a function of the grain orientation [14]. A measurement in transmission is used in a water tank. The emitter is a 1/2" in diameter wideband transducer of 2.25 MHz central frequency, and the receiver is a hydrophone.
The welded samples were cut in a flat position and shielded metal arc welding mock-up. The samples are considered macroscopically homogeneous and orthotropic. The real orientations that are obtained are 0°, 10°, 35°, 45°, 60°, 80° and 85° relatively to the normal to the samples surface. Samples are placed in the farfield of the emitter. The beam decomposition into plane waves angular spectrum is used to correct the effects of beam divergence [15]. With this approach, deviations and mode conversions could be taken into account. The hydrophone scans a plane $z=z_o$ parallel to the emitter surface and acquires a signal $s(t,x,y,z_o)$ at each point (x,y). The angular frequency spectrum $S(x,y,\omega_o,z_o)$ is

calculated for each signal by Fourier-transform. For an angular frequency ω_o, a 2D spatial Fourier-transform gives the so called plane waves angular spectrum $U(kx,ky,\omega_o,z_o)$ in the k-space domain. Firstly the incident field is mapped without any sample. The hydrophone moves in the plane containing the front face of the sample ($z_o=0$). Then the sample is inserted and the transmitted field is mapped in a second plane in the proximity of the sample's back face ($z_o>d$). For the angular frequency ω_o corresponding to a frequency of 2.25MHz, the plane waves angular spectra $U(kx,ky,\omega_o,z_o=0) = U_{inc}$ and $U(kx,ky,wo,z_o=d+\varepsilon) = U_{tra}$ are calculated. A "semi-theoretical" transmitted plane waves angular spectrum U'_{tra} is obtained by multiplying experimental U_{inc} with the transmission coefficients calculated in the k-space domain.

Transmission coefficients computation was solved in the orthotropic case [15] and was then extended to the monoclinic case. In fact the elastic description of an orthotropic material disorientated according to an axis of the fixed coordinate system becomes monoclinic. So, except for samples with 0° and 90° grain orientation that present an orthotropic description, all other samples are described as monoclinic materials. For some samples a deviation in two directions is observed (sample 10°). It confirms the result of the first study where little deviation in plane SV are observed (§ 4). If these two deviations are considered, the material exhibits triclinic elastic properties for the ultrasonic beam. Transmitted coefficients have to be calculated for this case. The attenuation for each direction of propagation (kx,ky) is calculated by comparing simulated transmitted beam and real one. The attenuation is expressed as the ratio between the experimental transmitted energy and the theoretical transmitted energy.

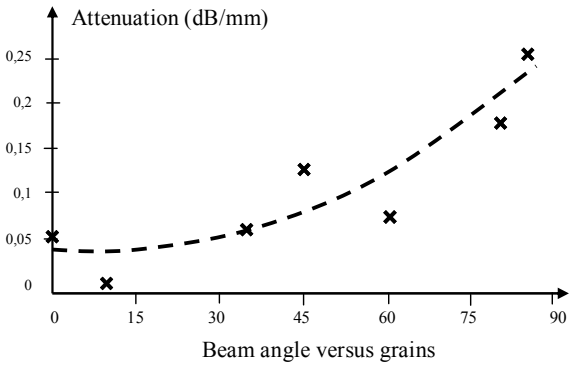

Figure 4. Experimental results of attenuation

Experimental results in figure 4 are in good agreement with theoretical calculations using Ahmed's modelling [16]. The double correction of beam deviation is used to obtain a good transmitted energy. This double correction reveals to be important for the 0° sample as a grain deviation in SV plane of about

5° was observed. With this correction a global monotonic increase of the attenuation is observed. Without this correction the attenuation value at 0° would be equal to 0,18 dB/mm. This result confirms once more that it is valuable to describe precisely the material. Slight 3D disorientations may give significant variations in the UT modelling. In part 4, it was observed that such order of 3D disorientations is possible for welding in position.

6 Inverse methodoly

The inverse problems are nowadays regularly encountered in the field of ultrasonic nondestructive testing [17]. The principle consists in comparing data obtained from experimental measurements with those obtained from a mathematical model known as the direct model. Results depend on the parameters assigned to the model (parameters of interest p). In this study the direct model corresponds to the coupling of MINA and ATHENA. The parameters of interest (input data) are the remelting and pass inclination parameters $p = (R_L, R_V, \theta_B, \theta_C)$. The output data is the full transmitted echodynamic curve at the bottom of the weld. The echodynamic curve corresponds to the maximum wave amplitude measured by a receiver scanning the bottom of the weld. In the interest of sensitivity, five transmitter positions are used so that the ultrasonic beam crosses most of the weld. The dissemblance criterion used to quantify the comparison is the estimator in the least squares sense.

Current ATHENA code does not yet take the attenuation into account. As a consequence, the amplitudes of the echodynamic curves simulated by ATHENA and those of the experimental curves can notably differ. Inversion of experimental data is not possible at this time. To overcome this difficulty experimental data are obtained by simulation using MINA and ATHENA. The main advantage is that the inversion can be done without the errors inherent in experimental measurements. All the parameters are completely known. The sensitivity of the cost function J and the presence of local minima can be studied in that case. This process is a useful first step before inversion with real data to demonstrate that a model is sufficiently well established to be inversible. Figure 5 shows an example of the evolution of the estimated parameters.

The genetic algorithm GA-Toolbox from MATLAB® is used. The main algorithm parameters are therefore the population size (N), the number of bits used to code parameters (Preci), the crossover rate (0<PcCros<1) and the replacement rate (0<Ggap<1). The tournament selection and the double point crossover are used. The search domain must be well-defined. These limits have been determined for each parameter experimentally from macrographs. This gives a realistic precision of the parameters.The inversion solution is found in commonly 16 generations, for a computation time of 4 hours on a Pentium IV @2.4 GHz [17]. The estimated parameters $R_L = 0.471$, $R_V = 0.263$, $\theta_B = 18.18°$ and $\theta_C = 12.25°$ are independent from the initialisation and are very close to the solution.

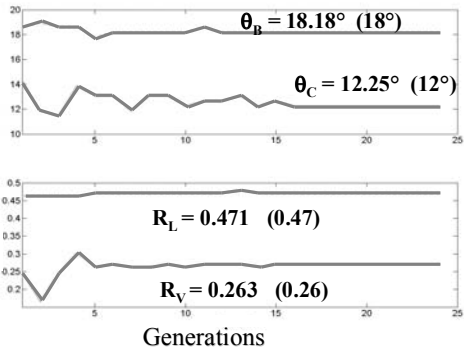

Figure 5. Inverse Methodology Results

The demonstration is done that inversion of this kind of direct problem is now possible.

7 Conclusion

Several advances in the field of ultrasonic modelling are presented. They are related to the ultrasonic testing of austenitic stainless steel welds which were reputed to be very difficult to be qualified by ultrasound. Advances were conducted with the intention to model the complete ultrasonic beam propagation in multi-pass welds. The foundation of all these advances is to be able to have a good material description for wave propagation. The MINA model allows a solid foundation regarding this objective. In this paper new elements are brought to enlarge the range of application of the MINA model. Another important element for the material description is a good evaluation of the attenuation, a solution for accurate measurement is presented and results are in good agreement with modelling. The direct model is settled using MINA and ATHENA. The inverse crime is solved; as a result it demonstrates the soundness of this coupling.
Further prospects are planned. The first one is related to an inversion which takes into account experimental data. Future works are planned with the new ATHENA code taking attenuation into account. A second immediate prospect is to use this inversion method to verify the sequencing order of the passes. The order of passes is used in the MINA model to calculate the value of θ_B and θ_C parameters. Several modelling results demonstrated that there is a great influence of this sequencing order in the final resulting grain structure. Ultrasonic testing of complex welds may now be studied using this direct model as [19].

Acknowledgments : All the works presented in this paper were supported by Electricité de France (EDF).

References

[1] B. Chassignole, D. Villard, M. Dubuget, J.C. Baboux, R. El Guerjouma, 'Characterization of austenitic stainless steel welds for ultrasonic NDT', Review of Progress in QNDE, Vol.20, 2000, pp.1325-1332.

[2] J.A. Ogilvy, Computerized ultrasonic ray tracing in austenitic steel, NDT&E International 18 (2) (1985) 67–77.

[3] V. Schmitz, F. Walte, S.V. Chakhlov, 3D ray tracing in austenite materials, NDT&E International 32 (1999) 201–213.

[4] S. Halkjaer, M.P. Sorensen, W.D. Kristensen, The propagation of ultrasound in a austenitic weld, Ultrasonics 38 (2000) 256–261.

[5] K.J. Langenberg, R. Hannemann, T. Kaczorowski, R. Marklein, B. Koehler, C. Schurig, F. Walte, Application of modeling techniques for ultrasonic austenitic weld inspection, NDT&E International 33 (2000) 465–480.

[6] M. Spies, Elastic waves in homogeneous and layered transversaly isotropic media: plane waves and Gaussian wave packets. A general approach, JASA 95 (1994) 1748–1760.

[7] M. Spies, Modeling of transducer fields in inhomogeneous anisotropic materials using Gaussian beam superposition, NDT&E International 33 (2000) 155–162.

[8] X. Zhao, S.J. Song, H.J. Kim, T. Gang, S.C. Kang, Y. H. Choi, K. Kim, S.S. Kang, Determination of incident angle and position of optimal mode ultrasonic beam for flaw detection in anisotropic and inhomogeneous weldments by ray tracing, J. of the Korean Society for Nondestructive Testing, Vol. 27, N°3, 2007, pp 231-238

[9] A. Apfel, J. Moysan, G. Corneloup, B. Chassignole, Simulations of the influence of the grains orientations on ultrasounds, 16th WCNDT, Montreal, 2004

[10] A. Apfel, J. Moysan, G. Corneloup, t. Fouquet, B. Chassignole, Coupling an ultrasonic propagation code with a model of the heterogeneity of multipass welds to simulate the ultrasonic testing. Ultrasonics, Volume 43, Issue 6, May 2005,pp 447-456

[11] B. Chassignole, Influence of the Metallurgical Structure of Austenitic Stainless Steel Welds on the Ultrasonic Non Destructive Testing, PhD Thesis, ISAL 0107, 2000, 207 p (fr).

[12] J. Moysan, A. Apfel, G. Corneloup, B. Chasssignole, Modelling the Grain Orientation of Austenitic Stainless Steel Multipass Welds to Improve Ultrasonic Assessment of Structural Integrity, International Journal of Pressure Vessels and Piping, Vol. 80 n°2, 2003, pp 77 - 85

[13] T. Seldis, C. Pecorari, M. Bieth, Measurements of longitudinal wave attenuation in austenitic steel, 1st International Conference on NDE in Relation to Structural Integrity for Nuclear and Pressurised Components, Amsterdam (Netherlands), 1998, pp 769-777.

[14] M.A. Ploix et al., Attenuation Assessment for NDT of Austenitic Stainless Steel Welds, 9 th European Conference on NDT, Berlin, 25-29 sept. 2006

[15] B. Hosten, Reflection and Transmission of Acoustic Plane Waves on an Immersed Orthotropic and Viscoelastic Solid Layer, JASA, Vol. 89, No. 6, 1991, pp. 2745-2752

[16] S. Ahmed and R.B. Thompson, Propagation of elastic waves in equiaxed stainless-steel polycrystals with aligned [001] axes, J. Acoust. Soc. Am. 99, 1996, 2086-2096.

[17] G. Haïat, P. Calmon, A. Lhémery, F. Lasserre, A model-based inverse method for positioning scatterers in a cladded component inspected by ultrasonic waves, Ultrasonics, Vol. 43 (8), 2005, p.619-628.

[18] C. Gueudré, L. Le Marrec, J. Moysan, B. Chassignole, Ultrasonic data inversion for characterization of heterogeneous welds, Conf. COFREND 2008, Toulouse, 20-23 May, 2008

[19] B. Chassignole, O. Paris, E. Abittan, Ultrasonic examination of a CVCS weld, 6th ICNDE, Budapest, 8 – 10 October 2007

http://www.springer.com/978-3-540-89104-8

Ultrasonic Wave Propagation in Non Homogeneous Media

Leger, A.; Deschamps, M. (Eds.)
2009, X, 435 p. 168 illus., Hardcover
ISBN: 978-3-540-89104-8